Noncircular Wigner–Seitz Cells in Strongly Segregated Block Copolymers

Glenn H. Fredrickson

Departments of Chemical and Nuclear Engineering and Materials, University of California, Santa Barbara, California 93106

Received February 16, 1993; Revised Manuscript Received April 29, 1993

ABSTRACT: A perturbation method is developed that allows for the systematic calculation of the elastic free energy of block copolymer microphases and goes beyond the approximation of a circularly (or spherically) symmetric Wigner–Seitz cell. The method is applicable in the limit of strong segregation between dissimilar blocks and to any type of microphase or copolymer architecture. As a demonstration of its utility, I perform an explicit calculation of the elastic free energy for the hexagonal microphase of diblock copolymers. In the composition window where this microphase is observed, I show that the circular cell approximation of Semenov underestimates the elastic energy of the corona by no more than 6%.

I. Introduction

Block copolymers have received much attention in recent years due to the broad range of materials properties that can be achieved, as well as the precise control that can be exercised over such properties by tailoring chain architecture, composition, and molecular weight at the time of synthesis.[1,2] Besides the practical interest in copolymeric materials for applications such as adhesives, compatibilizers, and thermoplastic elastomers, block copolymers exhibit a rich variety of phase transformations, critical phenomena, and unusual rheological properties. As a result, these materials have been used as model systems for studying fluctuation effects on equilibrium[3] and nonequilibrium[4] order–disorder phase transitions.

Simple A–B diblock copolymers, consisting of linear chains formed by covalently bonding a type-A homopolymer to a type-B homopolymer, self-assemble in the melt to produce a variety of microphase structures in which the A-blocks are spatially segregated from the B-blocks.[1,2,5,6] These microphases are spatially-periodic composition patterns that can belong to one of several crystallographic classes. The most commonly observed phases are lamellae, hexagonally-packed cylinders, and body-centered-cubic arrays of spheres. At low temperature or high molecular weight, the so-called strong aggregation limit (SSL) where the A- and B-blocks are highly incompatible, only one additional phase, the ordered bicontinuous double diamond phase (OBDD),[6,7] has been postulated as an equilibrium microphase structure. The OBDD phase belongs to the space group $Pn3m$, and its unit cell is bisected by a connected triply-periodic surface that has approximately constant mean curvature.

To a good approximation in the SSL, phase boundaries are independent of both temperature and molecular weight.[8,9] Thus, copolymer composition f (the volume fraction of the A-block) is the primary variable under synthetic control that can be used to influence morphology in diblock copolymers. Lamellar phases are generally observed for compositionally symmetric copolymers, $f = {}^1/_2$. By increasing the asymmetry of the copolymers, e.g. by lowering f, it is possible to observe a hexagonal phase in which the A-blocks fill the insides of hexagonally packed cylinders. The OBDD phase has been reported in a narrow band of compositions intermediate between those that produce lamellar and hexagonal microphases. The spherical phase (body-centered-cubic packing of type-A spheres) is observed at the lowest values of f.

Theories for the SSL of diblock copolymers[8,9] have been quite successful at reproducing the experimentally observed transitions between the classical microphase structures (lamellae, cylinders, and spheres) on varying f. However, there is presently no satisfactory theory that explains the existence of the OBDD structure as an equilibrium microphase. The most detailed calculation to date[10] fails to predict the thermodynamic stability of the OBDD phase in the composition range where it has been observed experimentally. Other attempts[11] to predict the low-temperature stability of a perforated lamellar phase observed near the order–disorder transition in polyolefin diblock copolymer melts[5] have also been unsuccessful.

A frequently invoked approximation,[8,9,11] when such theoretical calculations are performed, is to replace the exact Wigner–Seitz cell of the periodic structure by a circularized (or sphericalized) cell of higher symmetry (see, e.g., Figure 1). This procedure greatly simplifies analysis in the SSL but generally leads to an underestimate of the elastic free energy. Because the free energy differences between microphases are very small, accounting for the inability of calorimetric methods to provide information on structural transitions in block copolymers, it has been suggested that very accurate calculations on the complete Wigner–Seitz cells of competing structures might be necessary to predict the stability of bicontinuous phases. As a first step along these lines, I explore in the present paper the accuracy of the circularization approximation for the Wigner–Seitz cell of the classical hexagonal microphase. This is a particularly important test case, because the OBDD and perforated lamellar phases have been observed at compositions between cylinders and lamellae. Moreover, no circularization is necessary for the lamellar phase unit cell.[9] Hence, by performing such a calculation for the hexagonal phase, it will be possible to estimate how accurately the free energies of bicontinuous phases must be computed in the SSL to assess their stability relative to lamellae and cylinders.

My approach resembles an electronic structure calculation for a metal but utilizes only classical elasticity theory. In particular, I exploit a previous finding[12] that the elastic free energy of a deformed, molten polymer brush can be obtained by modeling the layer as an isotropic elastic medium with a shear modulus proportional to the square of the number of grafted chains per unit area. The method can be easily generalized to other microphase structures, e.g. to the Wigner–Seitz cell for body-centered-cubic

0024-9297/93/2226-4351$04.00/0

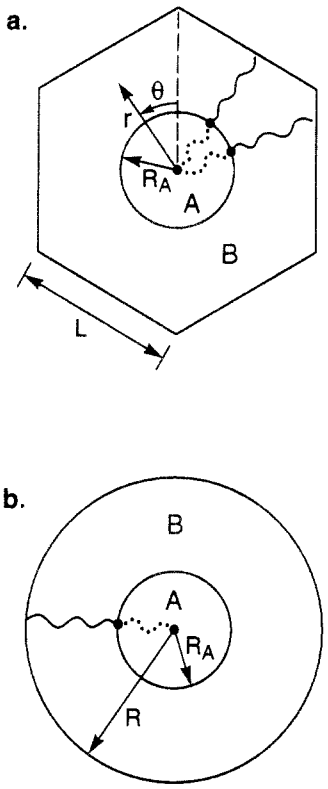

Figure 1. (a) Wigner–Seitz cell of the hexagonal phase of diblock copolymers. The cell has sides of length L that serve as the outer boundary of the corona region. The type-A blocks occupy the core region, $r < R_A$, which constitutes a fraction f of the total cell volume. In the analysis of section III, I utilize conventional polar coordinates (r,θ) as shown in the figure. (b) Circular approximation to the Wigner–Seitz cell. The outer boundary of the corona is approximated by a circle of radius R that encompasses the same area as a hexagon of side L (see eq 2.1).

spheres, and to other block copolymer architectures. It may also have applications to related problems in polymer and colloid science involving end-grafted or end-adsorbed polymer chains swollen by a solvent.

In the next section I review the computation of the SSL elastic free energy for the hexagonal phase of diblock copolymers in the circular Wigner–Seitz cell approximation. In section III.A I introduce the perturbation method used to correct the corona (cylinder exterior) free energy to properly account for the hexagonal unit cell. Explicit results are given in section III.B. Finally, in section IV I discuss the implications of the results for the SSL phase diagram.

II. Hexagonal Phase in the Circular Approximation

In the present section I consider an incompressible melt of A–B diblock copolymers, self-assembled into a hexagonal phase of cylinders with the A-blocks on the interior of each cylinder. For simplicity, the chains are assumed to consist of a block of Nf type-A monomers bonded to a block of $N(1 - f)$ type-B monomers, each monomer occupying a volume v and having a statistical segment length a. I adopt the conventional definition of segment length, whereby the unperturbed mean-squared radius of gyration is given by $Na^2/6$. The product of the Flory chi parameter for the A–B pair, χ, and the total degree of polymerization, N, is a measure of the degree of incompatibility between blocks that can be used to distinguish regimes of strong and weak segregation.[1] Here I restrict consideration to the strong segregation limit (SSL) for which $\chi N \gg 10$. Under such conditions the cylinder cores contain almost exclusively type-A monomers and the coronas (regions surrounding each cylinder) are almost pure B.

The unit (or Wigner–Seitz) cell for the hexagonal microphase is shown in Figure 1a. In this cell, the A-blocks are assumed to occupy a cylindrical core of radius R_A and the B-blocks fill in the remainder of the hexagonal cell with sides of length L. The circular approximation for the Wigner–Seitz cell adopted by previous workers[8,9] is shown in Figure 1b. This approximation is effected by replacing the hexagonal corona boundary by a cylinder of radius R chosen to enclose the same volume:

$$R = \left(\frac{3\sqrt{3}}{2\pi}\right)^{1/2} L \approx 0.90939L \tag{2.1}$$

This circular approximation has the virtue of imparting axial symmetry on the self-consistent field theory that is used to compute the elastic free energy.[8,9] The field equations thus reduce to simpler equations in only a single radial coordinate.

In the SSL, the free energy of the circular cell in Figure 1b can be written simply as a sum of three terms

$$F = F_A + F_B + F_I \tag{2.2}$$

where F_A is the elastic (i.e. chain stretching) free energy of the cylindrical core of radius R_A, F_B is the elastic free energy of the annular corona region, and F_I is the interfacial free energy of the A–B core–corona interface. This final quantity can be expressed as the product of the interfacial area with an interfacial tension, γ:

$$F_I = 2\pi R_A H\gamma \tag{2.3}$$

Here, H is the length of the cylinder and I note that the interfacial tension is approximately composition-independent,[8,9] $\gamma \sim k_B T\chi^{1/2}a/v$.

In the extreme SSL, achieved for $\chi N \to \infty$, Semenov[9] has demonstrated that the elastic free energy of the core region can be rigorously obtained by neglecting the fluctuations of the chain trajectories about their classical (i.e. most probable) paths. This simplification avoids the numerical intricacies of the self-consistent field theory developed by Helfand[8] and permits a compact analytical expression for the asymptotic SSL core energy. Semenov's result, which explictly accounts for a nonuniform distribution of chain ends, can be written

$$\beta F_A = \frac{\pi^3}{16}\frac{R^4 H}{a^2 v N^2} \tag{2.4}$$

where I note the relation $R_A^2 = fR^2$ and the definition $\beta \equiv 1/k_B T$.

An analytic expression[13] is also available for the elastic free energy of the corona in the SSL that accounts for the exclusion of B-block free ends from a region near the A–B interface at $r = R_A$ (the so-called "dead zone"). This exact expression, however, is quite complicated and has been shown[13] to be closely approximated by a simpler expression that results from the Alexander–de Gennes assumption that all free ends of the B-blocks lie at the outer surface of the corona ($r = R$).[9,14] The approximation can be written

$$\beta F_B = \frac{3\pi}{8}\frac{R^4 H}{a^2 v N^2}\ln(1/f) \tag{2.5}$$

To complete the calculation of the free energy in the circular approximation, I combine the three portions of the free energy according to eq 2.2 and divide by the total cell volume $\pi R^2 H$ to obtain a free energy density F_V. On

minimization with respect to R, one recovers Semenov's result

$$R^3 = \frac{16\beta\gamma v f^{1/2} a^2 N^2}{\pi^2 + 6\ln(1/f)} \tag{2.6}$$

demonstrating the SSL scaling of the primitive cell size, $R \sim N^{2/3}$, and

$$F_V = 3f^{1/2}\gamma/R \tag{2.7}$$

It proves convenient to normalize this expression for the free energy density of the hexagonal phase by the free energy density of the lamellar phase, which is composition-independent in the SSL.[9] The result can be written

$$G_c(f) \equiv F_{V,hex}/F_{V,lam} = \frac{(2f)^{1/3}}{\pi^{2/3}}[\pi^2 + 6\ln(1/f)]^{1/3} \tag{2.8}$$

where the subscript on G_c denotes the circular approximation to the Wigner–Seitz cell.

The lamellae to hexagonal phase transition occurs in the present approximation at a composition where $G_c(f) = 1$. Numerically, this corresponds to a composition $f \approx 0.28$. Thus, lamellae are predicted to be stable for $0.28 < f \leq 0.50$ and the hexagonal phase is stable below $f = 0.28$ in the circular approximation. It should also be noted that a subsequent first-order phase transition from the hexagonal phase (circular cell) to the bcc spherical phase (spherical cell) is predicted to occur at $f = 0.12$.[9]

III. Analysis of Noncircular Wigner–Seitz Cells

A. General Approach. Next, I consider how to correct the calculation just outlined to properly account for a noncircular Wigner–Seitz cell, e.g. Figure 1a. My basic assumption is that the difference in free energy between Figure 1a and 1b is simply due to an additional elastic distortion of the corona and is not a result of changes in the core or interfacial energies. This of course is an approximation, since there will in general be a nonuniform distribution of block junction points around the A–B interface in Figure 1a. However, because the amplitude of the elastic distortion of the cell in Figure 1b to produce the cell in Figure 1a is small (see eq 3.10 below) and the A–B surface energy is large, I expect that these core and interfacial free energy changes will be negligible. Indeed, extensive microscopy on hexagonally ordered diblock samples has provided no evidence of core distortion. My second major assumption is that, as in the circular calculation outlined in the last section, the corona can be accurately modeled by the Alexander–de Gennes approximation of demanding that all B-block ends terminate at the outer surface of the Wigner–Seitz cell. Because this was explicitly demonstrated[13] to be numerically accurate for the circular cell and the elastic strains required to distort Figure 1b into Figure 1a are small, the Alexander–de Gennes approximation should be adequate for the present purposes.

With these approximations, my task is to compute the elastic free energy associated with distorting (stretching) the B-blocks in a circular corona into a hexagonal shape. In principle, this could be done by solving the self-consistent field equations derived by Helfand[8] in a two-dimensional cell. However, a simpler approach is possible if it is recognized that the elastic distortion (i.e. strain) is small. In particular, a recent study of surface modes on molten polymer brushes[12] unearthed a new perturbation technique for computing the energy required to distort the upper boundary of a flat Alexander–de Gennes brush. An important finding was that the elastic energy stored in a weakly deformed melt brush could be computed very simply by using classical linear elasticity theory[15] for an isotropic, incompressible medium with a shear modulus given by

$$\mu = 3\,k_B T v\sigma^2/a^2 \tag{3.1}$$

In this equation, σ is the number of chains per unit area grafted to the flat substrate of the brush. I can generalize this expression to describe the shear modulus of the circular corona layer shown in Figure 1b by simply replacing σ by a radially varying number of chains per unit area (r is measured from the center of the core):

$$\sigma(r) = \frac{Q}{2\pi r H} = \frac{R^2}{vNr} \tag{3.2}$$

Here Q is the number of block copolymers contained in the unit cell shown in Figure 1b. Combining eqs 3.1 and 3.2 leads to an r-dependent shear modulus that can be written

$$\mu(r) = \mu_0(R/r)^2 \tag{3.3}$$

where the shear modulus at the outer circular boundary of the corona ($r = R$) is given by

$$\mu_0 = \frac{3}{4}k_B T\frac{R^2}{va^2N^2} \tag{3.4}$$

I thus model the cylindrical corona in Figure 1b as an isotropic elastic medium with a nonuniform shear modulus given by eq 3.3. For the purpose of enforcing constant density in the layer, it also proves *convenient* to introduce a nonuniform bulk modulus, $K(r)$, of the form

$$K(r) = K_0(R/r)^2 \tag{3.5}$$

The limit of an incompressible corona can then be achieved by taking the limit $K_0/\mu_0 \to \infty$ at the end of our calculations.

The general problem of computing the elastic free energy associated with the distortion of a cylindrical corona into a hexagonal Wigner–Seitz cell thus amounts to a classical boundary value problem that can be stated as follows. I must solve for the elastic displacement field $\mathbf{d}$ satisfying the equilibrium condition

$$\nabla\cdot\Pi = 0 \tag{3.6}$$

where the elastic stress tensor Π is related to the strain tensor $\mathbf{u}$ by the constitutive equation[15]

$$\Pi = K\,\mathrm{tr}(\mathbf{u})\mathbf{I} + 2\mu\left[\mathbf{u} - \frac{1}{3}tr(\mathbf{u})\mathbf{I}\right] \tag{3.7}$$

In this expression, $\mathbf{I}$ is the unit tensor and I note that K and μ vary with position according to eqs 3.5 and 3.3. Moreover, the linear strain tensor $\mathbf{u}$ is related to the elastic displacement field $\mathbf{d}$ by the usual expression[16]

$$\mathbf{u} = \frac{1}{2}[\nabla\mathbf{d} + (\nabla\mathbf{d})^T] \tag{3.8}$$

The boundary conditions are simply that $\mathbf{d} = 0$ on the circular boundary at the A–B interface ($r = R_A$ in Figure 1) and that the radial component of $\mathbf{d}$ at the outer coronal surface is chosen to generate the prescribed hexagonal cell. Finally, I require that the elastic *shear* stress at the outer surface must vanish.

Having solved the boundary value problem just outlined and imposed incompressibility by taking the limit $K_0/\mu_0 \to \infty$ allows the elastic free energy of distortion to be readily constructed from the strain tensor. In particular, the

correction to the elastic free energy of the corona imposed by the hexagonal cell can be written

$$\Delta F_B = \int_{cell} dV\, \mu\, \mathrm{tr}(\mathbf{u}\cdot\mathbf{u}) \tag{3.9}$$

where the volume integral is over the corona of the Wigner–Seitz cell.

B. Perturbation Theory for a Hexagonal Cell. The boundary value problem just outlined can be conveniently solved in cylindrical coordinates (r, θ, z) by means of a perturbation technique. As the elastic stresses represent forces that act only in the (r, θ) plane, I subsequently work only in this two-dimensional space (see Figure 1). For the purpose of fomulating the perturbation theory, it proves convenient to develop the outer hexagonal boundary of the corona in a Fourier series. In particular, taking note of the relationship between R and L given in eq 2.1, the location of the outer boundary in Figure 1a, $r = R_H(\theta)$, can be expressed as

$$R_H(\theta)/R = 1 + \sum_{n=1}^{\infty} \epsilon_n \cos(n6\theta) \tag{3.10}$$

where

$$\epsilon_n = \left(\frac{24\sqrt{3}}{\pi}\right)^{1/2} \int_0^{\pi/3} d\theta \frac{\cos(n6\theta)}{\sin\theta + \sqrt{3}\cos\theta} \tag{3.11}$$

The first three coefficients are given numerically by

$$\epsilon_1 = 5.8102 \times 10^{-2}$$

$$\epsilon_2 = 1.6110 \times 10^{-2}$$

$$\epsilon_3 = 7.3316 \times 10^{-3} \tag{3.12}$$

Because the ϵ_n are small compared with unity, the elastic strains generated by the boundary perturbation will also be small. Hence, to leading order in ϵ_n, I can construct the general solution to the boundary value problem by superimposing solutions obtained for a pure harmonic distortion of the boundary. In particular, I need to solve for the displacement field components $d_r(r,\theta)$ and $d_\theta(r,\theta)$ satisfying eq 3.6 and subject to the boundary condition

$$d_r(R,\theta) = \epsilon_n R \cos(n6\theta) \tag{3.13}$$

The no-displacement boundary conditions at the A–B interface can be written

$$d_r(R_A,\theta) = d_\theta(R_A,\theta) = 0 \tag{3.14}$$

and the remaining no-shear–stress condition at the outer surface can be written to first order in ϵ_n as

$$\left(\frac{\partial d_\theta}{\partial r} - \frac{d_\theta}{r} + \frac{1}{r}\frac{\partial d_r}{\partial \theta}\right)_{r=R} = 0 \tag{3.15}$$

This boundary value problem can be easily solved with the ansatz

$$d_r(r,\theta) = \epsilon_n R \cos(n6\theta) C (r/R)^\lambda \tag{3.16}$$

$$d_\theta(r,\theta) = \epsilon_n R \sin(n6\theta) D (r/R)^\lambda \tag{3.17}$$

where C and D are constants to be determined by applying the boundary conditions. The eigenvalues, λ, are obtained by requiring that eqs 3.6–3.8 be satisfied. To leading order in $\mu_0/K_0 \ll 1$, this results in four permissible values of λ:

$$\lambda_1 = 1 + 6n$$

$$\lambda_2 = 1 - 6n$$

$$\lambda_3 = 1 + 2\sqrt{9n^2 + 1}$$

$$\lambda_4 = 1 - 2\sqrt{9n^2 + 1} \tag{3.18}$$

Corresponding to these eigenvalues are four values of $\kappa \equiv D/C$:

$$\kappa_1 = -(3n + 1)/(3n)$$

$$\kappa_2 = (3n - 1)/(3n)$$

$$\kappa_3 = -(1 + \sqrt{9n^2 + 1})/(3n)$$

$$\kappa_4 = -(1 - \sqrt{9n^2 + 1})/(3n) \tag{3.19}$$

Thus, to $O(\epsilon_n)$, the displacement field components can be written

$$d_r(r,\theta) = \epsilon_n R \cos(n6\theta) \sum_{i=1}^{4} C_i (r/R)^{\lambda_i} \tag{3.20}$$

$$d_\theta(r,\theta) = \epsilon_n R \sin(n6\theta) \sum_{i=1}^{4} C_i \kappa_i (r/R)^{\lambda_i} \tag{3.21}$$

The four coefficients $C_1, \ldots, C_4$ are determined by imposing the four boundary conditions, eqs 3.13, 3.14, and 3.15. This leads to the following set of linear equations:

$$\Sigma_i\, C_i f^{\lambda_i/2} = 0$$

$$\Sigma_i\, C_i \kappa_i f^{\lambda_i/2} = 0$$

$$\Sigma_i\, C_i = 1$$

$$\Sigma_i\, C_i[\kappa_i(\lambda_i - 1) - 6n] = 0 \tag{3.22}$$

This equation set is easily solved for specified values of copolymer composition, f, and harmonic order n, yielding $C_i = C_i(f,n)$.

The corrections to the elastic free energy of the corona follow from eq 3.9, which to leading order in ϵ_n, can be written

$$\Delta F_B = H \int_0^{2\pi} d\theta \int_{R_A}^{R} dr\, r\mu(r)[u_{rr}^2 + u_{\theta\theta}^2 + 2u_{r\theta}^2] \tag{3.23}$$

Substituting the representations 3.20 and 3.21 for the displacement field components into the strain components of eq 3.23, this free energy change reduces to

$$\beta \Delta F_B = \frac{3\pi}{8} \frac{R^4 H}{a^2 v N^2} \Phi(f) \tag{3.24}$$

where the function $\Phi(f)$ is defined by

$$\Phi(f) = 2\sum_{n=1}^{\infty} \epsilon_n^2 \sum_{i=1}^{4}\sum_{j=1}^{4} C_i C_j [1 - f^{(\lambda_i + \lambda_j - 2)/2}](\lambda_i + \lambda_j - 2)^{-1}[\lambda_i\lambda_j + (1 + 6n\kappa_i)(1 + 6n\kappa_j) + (1/2)(\kappa_i\lambda_i - \kappa_i - 6n)(\kappa_j\lambda_j - \kappa_j - 6n)] \tag{3.25}$$

In Table I, I provide numerical values for the function $\Phi(f)$ over a broad range of compositions. This function is

Table I. Numerical Values of the Function $\Phi(f)$ for a Range of Compositions, f[a]

f	$\Phi(f)$	f	$\Phi(f)$
0.00	0.0766	0.40	0.0837
0.05	0.0766	0.45	0.0889
0.10	0.0766	0.50	0.0967
0.15	0.0766	0.60	0.126
0.20	0.0768	0.70	0.197
0.25	0.0773	0.80	0.440
0.30	0.0784	0.90	2.52
0.35	0.0804	0.95	18.5

[a] The function is defined in eq 3.25.

slowly varying for $0 < f < 0.4$ and exhibits a weak divergence for $f \to 1$. Physically, however, I am only concerned with compositions for which cylinders are competitive with lamellae or spheres, i.e. $0.1 < f < 0.3$. According to Table I, $\Phi(f)$ varies only from 0.0766 to 0.0784 over this physical range of f. A composition of particular interest is $f = 0.28$, the location of the predicted lamellae to hexagonal phase transition. For this composition, I find $\Phi(0.28) = 0.0779$.

On the basis of the above perturbative calculation, I can now go back and correct the circular cell approximation for the corona free energy. By combination of eqs 2.5 and 3.24, the elastic free energy of the hexagonal corona shown in Figure 1a can be written

$$\beta F_B = \frac{3\pi}{8}\frac{R^4 H}{a^2 v N^2}[\ln(1/f) + \Phi(f)] \qquad (3.26)$$

For the compositions of physical interest, it is easily established from Table I that $\Phi(f)$ makes only a small correction to $\ln(1/f)$ in the above equation. For example, at $f = 0.28$, the hexagonal corona energy, eq 3.26, is only 6% larger than the circular corona energy, eq 2.5. To assess the effect of relaxing the circular approximation to the Wigner–Seitz cell on the lamellae–hexagonal phase boundary, it is a simple matter to generalize eq 2.8 to incorporate the corrected corona energy:

$$G_h(f) = \frac{(2f)^{1/3}}{\pi^{2/3}}\{\pi^2 + 6[\ln(1/f) + \Phi(f)]\}^{1/3} \qquad (3.27)$$

Here the subscript h denotes the hexagonal Wigner–Seitz cell. The lamellae to hexagonal transition, determined by the solution of the equation $G_h(f) = 1$, is thereby found to occur at $f = 0.27$. Hence, relaxation of the circular approximation leads to a small 4% reduction in the composition of the lamellae–hexagonal phase boundary.

IV. Discussion

In the above section I have shown that for strongly segregated diblock copolymers, the circular approximation for the Wigner–Seitz cell of the hexagonal phase is quite accurate. Although previous workers[8,9] had assumed this to be the case, my calculation provides explicit justification of this often-invoked approximation for the physical range of compositions where the hexagonal phase is observed, i.e. $0.1 < f < 0.3$. Specifically, I find that the elastic free energy in the circular approximation is about 6% too small at the lamellae–hexagonal phase boundary ($f = 0.28$), is 3% too small at $f = 0.1$, and is 14% too small at $f = 0.5$. Because the OBDD phase (or other constant mean curvature phases) would be expected at compositions intermediate between cylinders and lamellae, the failure of previous attempts[10,11] to predict the stability of such phases can likely not be ascribed to the sphericalization of the Wigner–Seitz cell.

In all of my calculations I invoked the Alexander–de Gennes approximation of restricting all chain ends to lie on the outer coronal surface. This restriction implies that my estimate of the SSL hexagonal phase free energy is actually an upper bound to the exact mean-field free energy in the limit $\chi N \to \infty$. Nevertheless, previous calculations on undistorted cylindrical phases[9,13] suggest that my result is actually a very close bound that is of sufficient accuracy to confidently address questions of phase stability.

The classical elasticity model and perturbation method described in the present paper can be easily extended to other microphase structures and to other copolymer architectures. For example, the Wigner–Seitz cell of the body-centered-cubic structure (spheres) could be analyzed by the methods outlined above. In such a case, the appropriate shear modulus corresponding to eq 3.3 would have a different r-dependence, i.e. $\mu(r) \sim r^{-4}$, and the cell boundary would be most conveniently developed in a spherical harmonic expansion. My calculation method for the SSL also does not rely on the copolymers having a diblock architecture. Ring–block copolymers, star–block copolymers, and linear–multiblock copolymers are all within the realm of the technique, although some modification of the shear modulus would be in order. Moreover, it may be necessary for certain architectures to account for a distribution of block lengths in the coronal region.

Acknowledgment. I am grateful to the Department of Chemical Engineering and Materials Science at the University of Minnesota for supporting my stay as a George T. Piercy Distinguished Visiting Professor. I am also grateful to Frank Bates for stimulating discussions that motivated this study. Partial support was provided by the National Science Foundation under PYI Grant NSF-DMR 9057147 and the Alfred P. Sloan Foundation.

References and Notes

(1) Bates, F. S.; Fredrickson, G. H. *Annu. Rev. Phys. Chem.* **1990**, *41*, 525.
(2) Goodman, I. *Developments in Block Copolymers*; Applied Science: New York, 1982 and 1985; Vols. 1 and 2.
(3) Bates, F. S.; Rosedale, J. H.; Fredrickson, G. H.; Glinka, C. J. *Phys. Rev. Lett.* **1988**, *61*, 2229.
(4) Koppi, K.; Tirrell, M.; Bates, F. S. *Phys. Rev. Lett.* **1993**, *70*, 1449.
(5) Hamley, I. W.; Koppi, K. A.; Bates, F. S.; Mortensen, K., Preprint.
(6) Thomas, E. L.; Alward, D. B.; Kinning, D. J.; Handlin, D. L.; Fetters, L. J. *Macromolecules* **1986**, *19*, 2197.
(7) Hasegawa, H.; Tanaka, H.; Yamasaki, K.; Hashimoto, T. *Macromolecules* **1987**, *20*, 1651.
(8) Helfand, E.; Wasserman, Z. R. In *Developments in Block Copolymers*; Goodman, I., Ed.; Applied Science: New York, 1982; Vol. 1.
(9) Semenov, A. N. *Sov. Phys. JETP* **1985**, *61*, 733.
(10) Anderson, D. M.; Thomas, E. L. *Macromolecules* **1988**, *21*, 3221.
(11) Fredrickson, G. H. *Macromolecules* **1991**, *24*, 3456.
(12) Fredrickson, G. H.; Ajdari, A.; Leibler, L.; Carton, J.-P. *Macromolecules* **1992**, *25*, 2882.
(13) Ball, R. C.; Marko, J. F.; Milner, S. T.; Witten, T. A. *Macromolecules* **1991**, *24*, 693.
(14) Leibler, L. *Makromol. Chem., Macromol. Symp.* **1988**, *16*, 1.
(15) Landau, L. D.; Lifshitz, E. M. *Theory of Elasticity*; Pergamon: New York, 1986; Vol. 7.
(16) Note that elastic displacements **d** in the hexagonal Wigner–Seitz cell are measured relative to material elements in the circular cell.